



## Analyzing observed or hidden heterogeneity on survival and mortality in an isogenic *C. elegans* cohort

Hitoshi Suda<sup>1</sup>, Tetsuji Shoyama<sup>1</sup> and Yuka Shimizu<sup>1</sup>

<sup>1</sup>Department of Biological Science and Technology, School of High-technology for Human Welfare, Tokai University, 317 Nishino, Numazu, Shizuoka, 410-0395, Japan

Received 25 May, 2009; accepted 29 September, 2009

**It is generally difficult to understand the rates of human mortality from biological and biophysical standpoints because there are no cohorts or genetic homogeneity; in addition, information is limited regarding the various causes of death, such as the types of accidents and diseases. Despite such complexity, Gompertz's rule is useful in humans. Thus, to characterize the rates of mortality from a demographic viewpoint, it would be interesting to research a single disease in one of the simplest organisms, the nematode *C. elegans*, which dies naturally under identically controlled circumstances without predators. Here, we report an example of the fact that heterogeneity on survival and mortality is observed through a single disease in a cohort of 100% genetically identical (isogenic) nematodes. Under the observed heterogeneity, we show that the diffusion theory, as a biophysical model, can precisely analyze the heterogeneity and conveniently estimate the degree of penetrance of a lifespan gene from the biodemographic data. In addition, we indicate that heterogeneity models are effective for the present heterogeneous data.**

**Key words:** aging, survival, mortality, observed heterogeneity, *C. elegans*, biodemography

An exponential index in Gompertz's mathematical model has often been used as an indicator of the aging rate<sup>1</sup>. However, there is some doubt about Gompertz's rule<sup>2–4</sup>.

Corresponding author: Hitoshi Suda, Department of Biological Science and Technology, School of High-technology for Human Welfare, Tokai University, 317 Nishino, Numazu, Shizuoka, 410-0395, Japan.  
e-mail: sudasai@wing.ncc.u-tokai.ac.jp

Recently, we proposed a diffusion theory (the so-called stochastic model) that can analyze quantitatively survival curves and the rates of mortality and examined the validity of the theory experimentally using the nematode *C. elegans*<sup>5</sup>. In addition, strong evidence that stochastic as well as genetic factors are significant in *C. elegans* aging has been found<sup>6</sup>. Thus, to examine the molecular mechanism behind aging and lifespan, our model is expected to serve as a useful analytical tool that can be used to extract information of a regulatory system from the survival or mortality curves. In this report, furthermore to demonstrate our model's validity, we mainly used a *C. elegans* mutant of the apoptosis-related *egl-1* gene, which loses its normal egg-laying function<sup>7</sup>. *C. elegans* has no heart, no blood vessels, no lungs, no liver, and no cancer. The body structure of *C. elegans* is very simple. Thus the number of diseases that worms catch is overwhelmingly smaller than that in humans. Under such a background, *C. elegans* is frequently used as an ultimate model animal for the research on aging. With this experimental system, the influence on the rates of mortality by a single disease with aging can be examined.

We first found that the biodemographic data of *egl-1* mutants have a heterogeneous feature. We observed that the origin of the heterogeneity is disease and aging. The *egl-1* mutant strain plays an important role in clearly distinguishing aging from the disease as a phenotype. Here, a typical example of observed heterogeneity is introduced. In addition, to support the validity of our model, we also employ two mutants; *ife-2* and *mev-1;fer-15*. The *ife-2* gene is related to protein synthesis<sup>8</sup>, and the *mev-1;fer-15* double mutant is oxygen-hypersensitive under highly oxidative stress<sup>5</sup>.

The data points of mortality in the used mutants clearly

deviate far from a single exponential curve that is calculated from the simplest Gompertz's expression. Thus we wondered whether Gompertz's rule can apply even to such odd behavior. To answer this question directly, we employ the heterogeneity theory of Vaupel and Yashin<sup>9</sup> and a discrete heterogeneity model<sup>10</sup> that extended the simplest Gompertz's formulation<sup>1</sup> to a theoretical framework applicable to a heterogeneous population. Using this crucial example, we examine whether the diffusion theory is more useful and convenient than the heterogeneity models. Furthermore, to find a biological meaning in heterogeneity, we focus on the estimation of the penetrance, which is a term used in genetics to describe the extent to which the properties controlled by a gene, its phenotype, are expressed. Here, we show that *egl-1* mutants have high penetrance.

## Materials and methods

### *C. elegans* strains

Strains were manipulated under standard conditions by Brenner<sup>11</sup>. We used the following three strains: MT1082 [*egl-1(n487)*], RB579 [*ife-2(ok306)*], and TK281 [*mev-1(kn1); fer-15(b26)*].

### Lifespan assays

The lifespan was conducted at 25°C or 20°C. Synchronized worms were grown on nematode growth medium (NGM) plates (90-mm diameter) with *E. coli* OP50 as a food source at 25°C after hatching ( $x=0$ ) and set up on NGM plates (35-mm diameter) after day 3; the starting population per plate consisted of 10–12 animals. Eggs of *egl-1* and *mev-1;fer-15* mutants were taken from young adults that had been grown on NGM plates at 16°C except for those of the *ife-2* mutant, which had been grown at 20°C. During egg laying, hermaphrodite animals were transferred daily to new NGM plates in order to prevent the contamination of adult populations by progeny up to the point when fertilization would not occur. The number of living and dead animals was scored daily until all animals no longer responded to gentle prodding with a platinum thin wire, at which time they were considered dead. Animals that died due to an extruded gonad or desiccation due to crawling on the edge of the dishes were censored and incorporated into the dataset. Worms that died were removed from the plates. For all lifespan measurements, assays were repeated at least three times. Data fitting of the fraction survival and mortality rates and statistical analysis were performed using KaleidaGraph software (version 3.6, Hulinks).

### Analytical models

#### Definitions of the mortality rate and the force of mortality

The fraction survival to age  $x$  is given by  $l_x=100\%$  ( $N_x/N_0$ ), where  $N_0$  and  $N_x$  are the initially set population number of animals and the number of animals alive on age  $x$ , respectively. The (age-specific) mortality rate  $q_x$  at age

$x$  ( $x \sim x+\Delta x$ ) is generally defined by

$$q_x = (l_x - l_{x+\Delta x})/(\Delta x l_x). \quad (1)$$

Since observations were conducted daily in the present measurements,  $\Delta x=1$ . Thus, our experimental mortality rate,  $q_x$ , may be given as follows:

$$q_x = (l_x - l_{x+1})/l_x. \quad (2)$$

$q_x$  is a discrete quantity, whereas the force of mortality,  $\mu_x$ , is in general defined as a continuous quantity as follows:

$$\begin{aligned} \mu_x &= -\frac{1}{N_x} \frac{dN_x}{dx} \\ &= -\frac{1}{l_x} \frac{dl_x}{dx} \left( = \lim_{\Delta x \rightarrow 0} \frac{l_x - l_{x+\Delta x}}{\Delta x l_x} \right) \\ &= -\frac{d}{dx} \log l_x. \end{aligned} \quad (3)$$

Thus, the force of mortality implies the limit of the mortality rate, i.e.,  $\Delta x \rightarrow 0$ , as well as  $N_0 \gg 1$ .

### A summary of the diffusion theory

We derived the equation of lifespan having a biological background on the basis of the diffusion differential equation as described in a previous paper<sup>5</sup>.

First, as the simplest case, in which individuals are genetically homogeneous and composed of a cohort, we reached the following solution:

$$\begin{aligned} l_x &= l_0(x, t_0) + (100 - l_0(x, t_0)) e^{-(x-t_0)^2/z^2} \\ l_0(x, t_0) &= \begin{cases} 100 & \text{at } x < t_0 \\ 0 & \text{at } x \geq t_0 \end{cases}, \end{aligned} \quad (4)$$

where  $z = \sqrt{4Dt_0}$ . Furthermore,  $D$  and  $t_0$  represent the fluctuation constant and the onset of demographic aging, respectively. Here, animals cultured under identically controlled circumstances, including temperature, nutrients, and lack of predators, are assumed to die of a single natural cause. The framework involved in the stochastic model is based on the existence of a regulatory system early in life and/or during adulthood. As a biological meaning of  $z$ , we have reported that the inverse of  $z$  is proportional to the physiological decline rate of respiration with age. Substituting Eq. 4 into Eq. 3, the force of mortality is written approximately as  $\mu_x \cong 2(x-t_0)/z^2$  at  $x \geq t_0$ . This expression corresponds to a special case of the Weibull model<sup>3</sup>.

For the case of  $n$ -causes of death, the extended version of Eq. 4 is given as follows:

$$l_x = \sum_i l_i(x), \quad (5)$$

where  $l_i(x) = l_{0i}(x, t_{0i}) + (l_{0i} - l_{0i}(x, t_{0i})) e^{-(x-t_{0i})^2/z_i^2}$ ,  $z_i = \sqrt{4D_i t_{0i}}$ ,

$l_{0i}(x, t_{0i}) = \begin{cases} l_{0i} & \text{at } x < t_{0i} \\ 0 & \text{at } x \geq t_{0i} \end{cases}$ , and  $\sum_i l_{0i} = 100$ . Substituting Eq. 5

into Eq. 3, the force of mortality may be expressed as

$$\mu_x = 2 \sum_i \frac{(x - t_{0i})}{z_i^2} \times \frac{l_i(x)}{l_x} \quad \text{at } x \geq t_{0i}. \quad (6)$$

### The Vaupel-Yashin model and a discrete heterogeneity model for a heterogeneous population

For simplicity, let us consider a heterogeneous population composed of two sub-cohorts in a single cohort. The average force of mortality,  $\langle \mu_x \rangle$ , is given by Vaupel and Yashin<sup>9</sup> as follows.

$$\langle \mu_x \rangle = \pi(x)\mu_1(x) + (1 - \pi(x))\mu_2(x), \quad (7)$$

$$\text{where } \pi(x) = \frac{\pi_0 p_1(x)}{[\pi_0 p_1(x) + (1 - \pi_0) p_2(x)]}, p_i(x) = \exp\left[-\int_0^x \mu_i(t) dt\right],$$

and  $i=1, 2$ .

Here, we employed the expression of Gompertz  $\mu_i(x) = A_i \exp(G_i x)$  to fit the rates of mortality because Vaupel and Yashin basically adopted Gompertz's rule to demonstrate their mathematical model. In addition,  $\pi_0$  represents the proportion of individuals who are in the first subcohort at time zero. Note that  $100 \pi_0$  corresponds to  $l_{01}$  in our biophysical model. Furthermore, to compensate for a weakness of the Vaupel-Yashin model, we discuss employing a discrete heterogeneity model<sup>10</sup> that developed from the Vaupel-Yashin model. The average fraction survival in the discrete heterogeneity model is expressed as

$$\begin{aligned} \langle l_x \rangle &= \sum_{i=1}^2 c_i p_i(x), \\ p_i(x) &= \exp\left[-\frac{A_i}{G_i} (e^{G_i x} - 1)\right], \\ \text{and } \sum_{i=1}^2 c_i &= 100. \end{aligned} \quad (8)$$

Here,  $c_1$  corresponds to  $l_{01}$  of our model.

## Results

### Observed heterogeneity in the *egl-1* mutant

The entire survival curve,  $l_x$ , of *egl-1* mutants at 25°C indicates a two-step-like shape (Fig. 1A). Indeed, we observed that about 90% of the population quickly died due to internal hatching of larvae or disease from day 3 to day 6 and the remainder died gradually of natural causes after day 6. The maximum lifespan was twenty days. The original survival curve could be clearly separated into two components after analyzing with the extended equation for lifespan, Eq. 5, and the addition of more components did not result in a better fit. At this time, the non-linear least-squares fitting method was used to statistically fit the equation of lifespan to the experimental values. Each theoretically isolated component, i.e., the first and the second modes, fitted each experimental component quite well (Fig. 1A). In this case, the first and second modes corresponded to the subcohorts of disease

and aging, respectively. In addition, the reconstructed curve from the two separated modes highly correlated with the entire original survival data (correlation coefficient 0.999; data not shown). The frequency,  $l_{01}$ , of the first mode represents the degree of penetrance of the *egl-1* gene. The reduced value is  $l_{01}/100 = 0.888$ , which is fully consistent with the observed value ( $482/543 = 0.888$ ), where the number of animals that died from disease and aging was 482 and 61, respectively. The z-value of the first and second modes was 0.98 and 5.70, respectively.

The rates of mortality,  $q_x$ , were calculated using Eq. 2. The experimental data clearly deviated from the linear relationship that would be expected from the simplest Gompertz's expression (Fig. 1B). The findings indicate that the mortality rates were convex early in life. We theoretically calculated the rates of mortality by substituting the fitting equation of reconstructed survival into Eq. 2; the rates are represented by  $q_x'$ . The predicted values,  $q_x'$ , from our model are quite compatible with the experimental values,  $q_x$  (correlation coefficient,  $r = 0.861$ ). Moreover, the force of mortality,  $\mu_x$ , which was calculated using Eq. 3, is superimposed on  $q_x$  in Fig. 1B. The  $\mu_x$  curve approximately fitted the  $q_x$  values and slightly deviated from  $q_x'$ . Furthermore, to verify whether Gompertz's rule is established in such a heterogeneous system, we fitted  $q_x$  using the Vaupel-Yashin model, which is composed of two components expressed by Gompertz's rule. As shown in Fig. 1C, the experimental values,  $q_x$ , are close to the fitting curve,  $\langle \mu_x \rangle$ . Here, the fitting parameters were chosen appropriately without using the maximum-likelihood method or the non-linear least-squares fitting method. Although these estimated parameters are not always unique, when we input  $\pi_0 = 0.50$ , the fitting curve fitted the data points well. The value of 0.50 that predicts the degree of penetrance of the *egl-1* gene is much lower than the observed value of 0.888. When the same value as the observed one was input into  $\pi_0$ , the fitting degree (correlation coefficient,  $r = 0.298$ ) was not better than that ( $r = 0.839$ ) at  $\pi_0 = 0.50$ . However, when we analyzed using the discrete heterogeneity model of Eq. 8, the degree of penetrance could be improved to 0.82. The entire survival data fitted the theoretical curve well, as shown in Fig. 1D.

### Effect of the temperature on the penetrance of the *egl-1* gene

To verify how the penetrance is influenced by an environmental factor, we investigated the effect of the temperature of the culture on the penetrance of the *egl-1* gene. Figure 2A shows the survival curve at 20°C. We could again observe two different phenotypes under this temperature condition. The maximum lifespan was seven days longer than that at 25°C. The proportion of animals catching the disease to the initial population was 0.683, where the number of diseased and aging animals was 192 and 89, respectively. This indicated a reduction of 30% from 0.888 at 25°C. The proportion of the first mode  $l_{01}/100 = 0.694$  that was obtained from

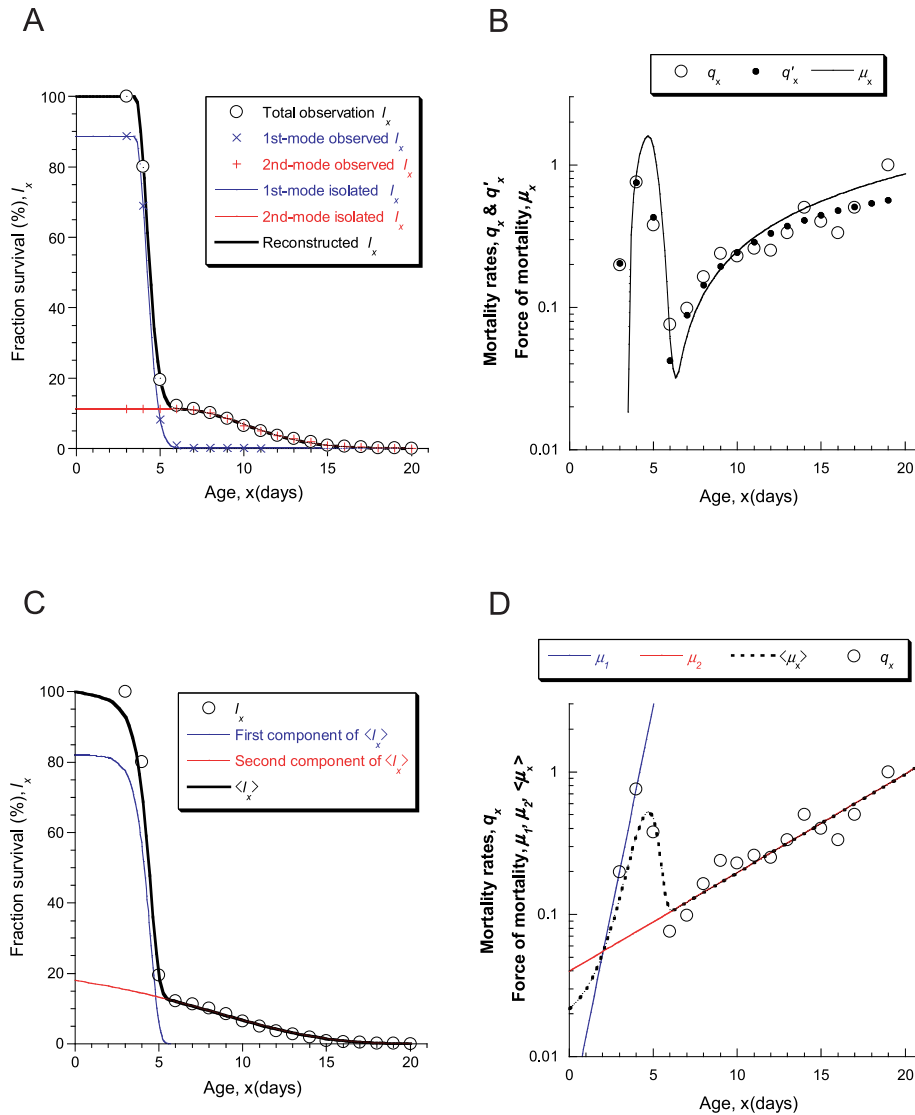


**Figure 1** Biodemographic data of the *egl-1* mutant cohort. (A) Survival; summed data from 5 trials, 543 animals at 25°C. Raw survival data consist of death due to a single disease (blue crosses, the number of worms;  $n=482$ ), senescence (red crosses,  $n=61$ ), and total data (open circles,  $n=543$ ). Blue, red, and bold black curves represent the fitting ones corresponding to each experimental data. The fitting parameters of the 1<sup>st</sup> mode were  $l_{01}=88.8$ ,  $t_{01}=3.5$ , and  $z_1=0.98$ , while those of the 2<sup>nd</sup> mode were  $l_{02}=11.2$ ,  $t_{02}=6.0$ , and  $z_2=5.70$ . (B) Mortality rates of (A).  $q_x$  indicates the experimental values (open circles);  $q'_x$ , the predicted mortality rates (filled circles);  $\mu_x$ , the force of mortality (—). (C) Analysis by the Vaupel-Yashin model. The fitting parameters in Eq. 7 were chosen as  $\pi_0=0.50$ ,  $A_1=0.00362$ ,  $A_2=0.03979$ ,  $G_1=1.34$ , and  $G_2=0.16$ . (D) Analysis by the discrete heterogeneity model. The fitting parameters in Eq. 8 were chosen as  $c_1=82.0$ ,  $c_2=12.0$ ,  $A_1=0.00036$ ,  $A_2=0.03979$ ,  $G_1=1.90$ , and  $G_2=0.16$ .

the analysis using our model is in good agreement with our observed value (0.683). On the other hand, the  $z$ -value of the first and second modes was 2.36 and 9.20, respectively.

As in the results at 25°C, the mortality data clearly deviated from the linear relationship that would be expected from the simplest Gompertz's equation (Fig. 2B). The profile of mortality,  $q_x$ , seems to be convex early in life. We calculated the rates of mortality,  $q'_x$ , expected from our model by substituting the fitting equation of reconstructed survival into Eq. 2. The predicted values,  $q'_x$ , are in quite good agreement with the experimental value,  $q_x$ . The force of mortality,  $\mu_x$ , is superimposed on  $q_x$  in Fig. 2B. The  $\mu_x$  curve fitted  $q_x$  and  $q'_x$

well. Moreover, to test the effectiveness of Gompertz's rule even in this heterogeneous system, we fitted  $q_x$  with the Vaupel-Yashin model. As shown in Fig. 2C, the experimental  $q_x$  values are approximately close to the fitting curve when the fitting parameters were chosen appropriately. Although these estimated parameters are not always unique, the experimental values fitted the theoretical curve calculated by  $\pi_0=0.694$  quite well. At this time, the  $\pi_0$  value was consistent with the observed value, 0.683.

#### Unobserved heterogeneity in the *ife-2* mutant

As shown in Fig. 3, similar data to those of *egl-1* mutants

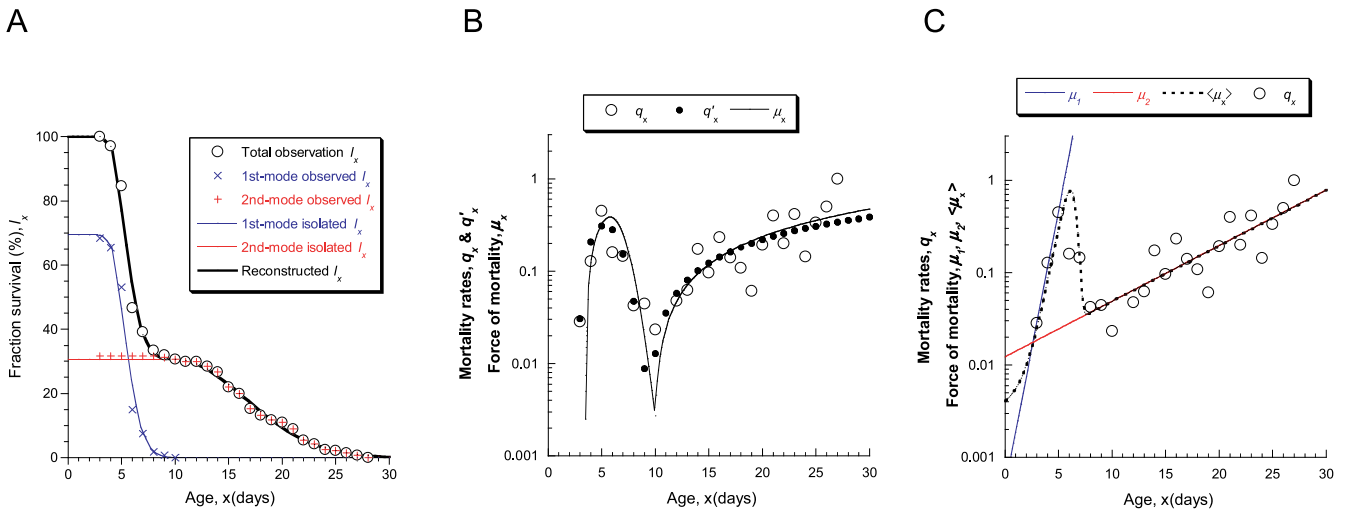


**Figure 2** Temperature effect on the biodemographic data of the *egl-1* mutant cohort. (A) Survival; data from a single trial, 281 worms, at 20°C. Raw survival data consist of death by a single disease (blue crosses,  $n=192$ ), senescence (red crosses,  $n=89$ ), and total data (open circles,  $n=281$ ). Blue, red, and bold black curves represent the fitting ones corresponding to each experimental data. The fitting parameters of the 1<sup>st</sup> mode were  $l_{01}=69.4$ ,  $t_{01}=3.5$ , and  $z_1=2.36$ , while those of the 2<sup>nd</sup> mode were  $l_{02}=30.6$ ,  $t_{02}=10.0$ , and  $z_2=9.20$ . (B) Mortality rates of (A).  $q_x$  indicates the experimental values (open circles);  $q'_x$ , the predicted mortality rates (filled circles);  $\mu_x$ , the force of mortality (—). (C) Analysis by the Vaupel-Yashin model. The fitting parameters in Eq. 7 were chosen as  $\pi_0=0.694$ ,  $A_1=0.00047$ ,  $A_2=0.012241$ ,  $G_1=1.38$ , and  $G_2=0.14$ .

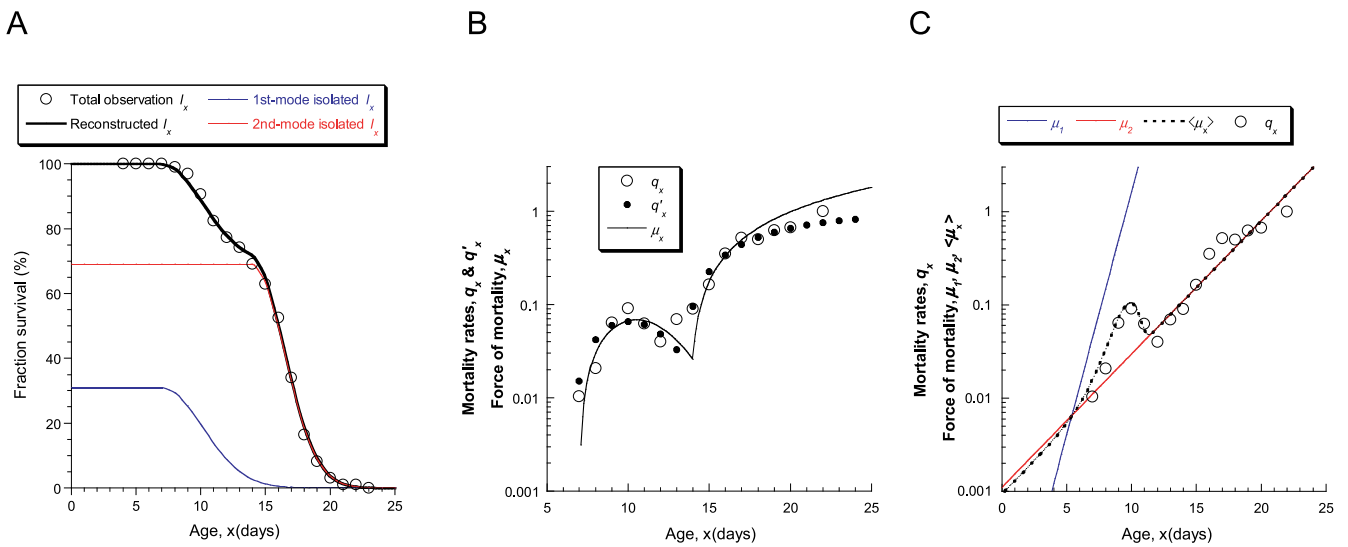


**Figure 3** Biodemographic data of the *ife-2* mutant cohort. (A) Survival in a single trial, 97 animals at 25°C. This strain was transferred from 20°C to 25°C after L1 larvae. The fitting parameters of the 1<sup>st</sup> mode (blue curve) were  $l_{01}=30.9$ ,  $t_{01}=7.0$ , and  $z_1=4.46$ , while those of the 2<sup>nd</sup> mode (red curve) were  $l_{02}=69.1$ ,  $t_{02}=14.0$ , and  $z_2=3.49$ . (B) Mortality rates of (A).  $q_x$  indicates the experimental values (open circles);  $q'_x$ , the predicted mortality rates (filled circles);  $\mu_x$ , the force of mortality (—). (C) Analysis by the Vaupel-Yashin model. The fitting parameters in Eq. 7 were chosen as  $\pi_0=0.15$ ,  $A_1=0.00001$ ,  $A_2=0.00110$ ,  $G_1=1.20$ , and  $G_2=0.33$ .

were obtained with another mutant of the *ife-2* gene. Differently from the case of the *egl-1* mutant, however, in this mutant, the reason for the two phases is unclear; in other words, it is a case of hidden heterogeneity, probably due to the low penetrance of the *ife-2* gene. The frequency of the first mode from our model was estimated to be 0.309.

As in the case of the *egl-1* mutant, the mortality data clearly deviated from the linear relationship that would be

expected from the simplest Gompertz's rule (Fig. 3B). The result indicates that the mortality rates,  $q_x$ , were convex early in life and later at older ages. We calculated the mortality rates,  $q'_x$ , obtained from our model by substituting the fitting equation of reconstructed survival into Eq. 2. The predicted  $q'_x$  from our model was quite consistent with the experimental value,  $q_x$ . Then, the force of mortality,  $\mu_x$ , was analyzed using Eq. 3 with the fitting parameters that were

determined through the curve fitting of the survival data.  $\mu_x$  is superimposed on  $q_x$  in Fig. 3B. The  $\mu_x$  curve fitted  $q_x$  and  $q'_x$  well. The slight deviation of  $\mu_x$  from  $q'_x$  seen at advanced ages is obviously caused by continuity or discreteness under the mathematical definition.

Furthermore, to examine the effectiveness of Gompertz's rule for this heterogeneity, we fitted  $q_x$  using the Vaupel-Yashin model. As shown in Fig. 3C, the experimental  $q_x$  values are in agreement with the fitting curve when the fitting parameters were chosen appropriately. Although those estimated parameters are not always unique, the fitting is good with experimental values at  $\pi_0=0.15$ . This is about half the value of 0.309 estimated by our model.

### Biodemographic data for the oxygen-hypersensitive *mev-1;fer-15* double mutant

Moreover, we tested our model employing the oxygen-hypersensitive double mutant *mev-1;fer-15* under highly oxidative stress (Fig. 4). When this mutant strain was exposed to a high oxygen concentration (90%) after maturation, its lifespan was remarkably shortened (Fig. 4A and ref. 5). The mortality rates,  $q_x$ , reached a complete plateau at advanced ages, as shown in Fig. 4B. Here, we first fitted the survival using the equation of lifespan, Eq. 4. Then we calculated the predicted mortality,  $q'_x$ , from our model by substituting the equation of survival with determined parameters in the previous step into Eq. 2. The  $q'_x$  values were in quite good agreement with the experimental  $q_x$  values, as seen in Fig. 4B. On the other hand,  $\mu_x$  was not at all coincident with  $q_x$  or  $q'_x$ . However, as the time interval  $\Delta x$  in Eq. 1 decreased from 1.0 to 0.05,  $q'_x$  gradually approached  $\mu_x$ , and both matched up completely at  $\Delta x=0.01$  (data not shown). This is a typical example that the rates of mortality do not always fit with the force of mortality because of the issues of  $q_x$ -discreteness and  $\mu_x$ -continuity.

## Discussion

### Observed heterogeneity and penetrance in *egl-1* mutants

A two-phase structure is revealed in biodemographic data, as demonstrated above. This heterogeneity probably results from the penetrance of the *egl-1* gene. Although our results suggest that an isogenic (100% genetically identical) population is composed of two subpopulations, we ascertained that the data did not result from mixing two different strains (data not shown). This means that the *egl-1* mutant cohort, despite being an isogenic population, has the capacity to generate a heterogeneous population. As pointed out by Vaupel and Yashin<sup>9</sup>, a heterogeneous population may consist of various homogeneous subpopulations. In particular, it must be noted that the heterogeneity of *egl-1* mutants could be observed as a phenotype without employing a special tool, such as a visualizing technique<sup>10</sup>.

If we compare the phenotype, the maximum lifespan, the  $t_0$  value and the z-value for the second component or mode

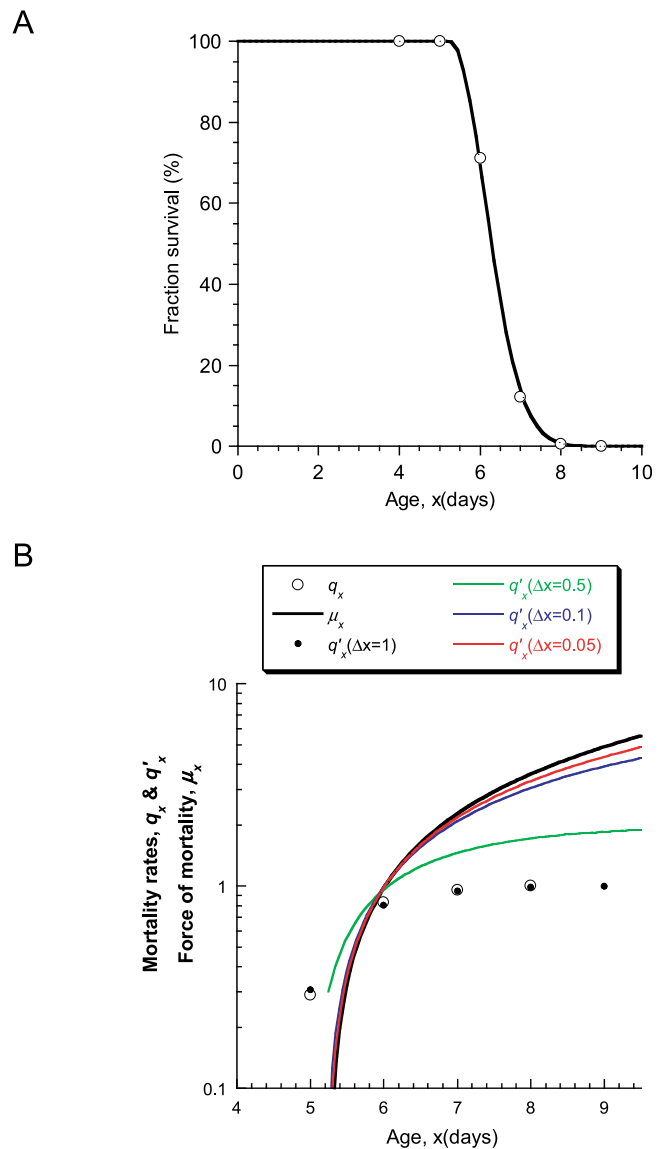


**Figure 4** Biodemographic data of the *mev-1;fer-15* double-mutant cohort at 25°C. (A) Survival of the *mev-1;fer-15* double mutant (360 animals, summed data from three trials) exposed to 90% oxygen concentration from day 4. The raw data were fitted by the non-linear least-squares method with Eq. 4, whose fitting parameters were determined as  $t_0=5.25$  and  $z=1.24$ . The bold black curve shows the fitting curve analyzed as a single mode. (B) Mortality rates of (A). The expected mortality rates  $q'_x$  from our model were calculated by substituting the fitting equation of survival determined at (A) into Eq. 1. Here, the interval time  $\Delta x$  in Eq. 1 was varied as 1.0 (filled circles), 0.5 (green line), 0.1 (blue line), and 0.05 (red line). The experimental  $q_x$  and predicted  $q'_x$  values are black circles and small black solid circles ( $\Delta x=1.0$ ), respectively. The bold black curve represents the force of mortality calculated from Eq. 6.

(red crosses) with those of the wild type<sup>5</sup>, it will be shown that the second component that died with aging has a very similar profile to that of the wild type. This similarity suggests that the second component in the *egl-1* mutant possesses a trait of the wild type.

When we reduced the temperature of the culture by 5°C

from 25°C as an environmental factor, the magnitude of penetrance of the *egl-1* gene decreased by about 30%. Simultaneously, the lifespan of the first component (blue crosses) and the maximum lifespan at 20°C were extended in response to a z-value about twice as large at 25°C. This result suggests that the reduction of the metabolic rate may cause the extension of the lifespan and penetrance because the z-value correlates the metabolic energy<sup>5</sup>.

### Unobserved heterogeneity in *ife-2* mutants

The existence of heterogeneity in the *egl-1* mutant was pointed out above. Likewise, the presence of heterogeneity in the *ife-2* mutant was shown. Unlike *egl-1* mutants, *ife-2* mutants have not been shown to have two distinct phenotypes. This is an example of unobserved heterogeneity lacking direct experimental evidence. Although details are not given in this work, in addition to the present used mutants, similar heterogeneity has been observed in mutants other than those used in the present study; such results will be reported elsewhere. Even if two or more phenotypes related to aging and lifespan have been not found in a *C. elegans* cohort, the diffusion theory as well as heterogeneity models suggests that a genetically identical population may be composed of various homogeneous subpopulations. Even if the original cohort cannot be divided into two or more subcohorts as a phenotype, hidden heterogeneity may be visualized using the green fluorescent protein first developed by Wu *et al.*<sup>10</sup>. Although a mathematical analysis technique depends on a chosen model, to separate each subcohort from all survival data is necessary as a first step. Subsequently, the hidden heterogeneity must be directly measured to support its existence. However, at this stage in our research, the assignment of each subcohort predicted in the *ife-2* mutant cohort remains a future task.

### Validity of Gompertz's rule and comparison with the diffusion model

Thus far, the effectiveness of the two-phasic Gompertz's rule and that of other models than the Gompertz's rule have been reported<sup>4,12-13</sup>. In this study, using the Vaupel-Yashin model<sup>9</sup>, we demonstrated whether Gompertz's rule is really sufficient even for the present heterogeneous examples. As seen in Figs. 1C, 2C, and 3C, the rates of mortality could be almost fitted by the heterogeneity theory, except for the finiteness of the solution ( $q_x$  or  $\mu_x \neq 0$ ) before  $t_{0i}$  of each component. The diffusion theory has been derived under the fundamental assumption that worms do not die until  $x=t_{0i}$ , that is,  $q_x=0$  or  $\mu_x=0$  ( $0 \leq x < t_{0i}$ ). The problem of whether  $q_x$  is zero or finite before  $t_{0i}$  seems to be essential in association with the existence of a regulation mechanism, such as sensing, switching, and memorizing the rate of mitochondrial respiration in early life<sup>14</sup>. To support our model with direct evidence, we have to evaluate whether this condition does not contradict the experimental facts. Indeed, we have never observed worms die at least before  $t_{0i}$ . If we had observed

some worms die before  $t_{0i}$ , we would not have excluded the possibility of the existence of another subcohort. This point is crucial in evaluating the validity of both the diffusion and heterogeneity theories. Thus, our model seems to be supported, in contrast to heterogeneity models, which contradict our experimental fact:  $q_x=0$  before  $t_{0i}$ .

### A desirable procedure of analysis for fitting the rates of mortality

The force of mortality has usually been used to analyze the rates of mortality<sup>1-4,9,10,13,15</sup>. However, our result obtained with the *mev-1;fer-15* double mutant suggests that we should not fit the mortality directly using a model equation for the force of mortality. If we fitted the mortality rates in Fig. 4B directly using a model equation of the force of mortality, we would be directly led to a wrong result. In other words, only if the rates of mortality could be approximately regarded as continuity could the force of mortality be used to analyze them directly. In particular, the case of a small number of animals, as well as long-lived animals in an experimental condition, for example mice, must be noted<sup>15</sup>. Accordingly, as a fundamental procedure, we recommend analyzing the rates of mortality in the following way. First, a survival curve should be fitted with a model equation, as described in Section 4.2. Subsequently, the mortality,  $q_x'$ , should be calculated on the basis of the definition equation, Eq. 2, by substituting the fitting parameters obtained from the previous step into the formulated survival equation, such as Eq. 5 or 8. Likewise, the force of mortality should be calculated on the basis of a definition equation, such as Eq. 6 or 7, by substituting the fitting parameters obtained from the previous step into a formulated survival equation, such as Eq. 5 or 8. However, even if the force of mortality,  $\mu_x$ , were analyzed according to the above procedure, if continuity were not held, a large deviation between  $q_x$  or  $q_x'$  and  $\mu_x$  would be generated. We would like to emphasize once again that  $\mu_x$  is a predicted value at the limit of  $\Delta t \rightarrow 0$  and/or  $N_0 \rightarrow \infty$ . Even if there is a large deviation between  $q_x$  or  $q_x'$  and  $\mu_x$ , it is not a logical error.

### Conclusion

In this work, it is demonstrated that the biodemographic data of *egl-1* and *ife-2* mutants reveal heterogeneity. In particular, the heterogeneity of the *egl-1* mutant can be observed as a phenotype without using a special tool, such as a visualizing technique, to evidence theoretically predicted hidden heterogeneity. This observation implies that the *egl-1* mutant has high penetrance. Our biophysical model, as well as the heterogeneity models, strongly supports the existence of hidden heterogeneity and its biological significance with experimental evidence.

## Acknowledgements

We thank Takami Ozaki for their assistance of our experiments. We also thank Prof. N. Ishii, the International *C. elegans* Gene Knockout Consortium and the *Caenorhabditis* Genetics Center, which is funded by the NIH National Center for Research Resources, for providing some nematodes strains used in this work. This work is dedicated to Osamu Suda.

## References

- Gompertz, B. On the nature and the function expressive of the law of human mortality, and on a new mode of determining the value of life contingencies. *Phil. Trans. R. Soc. Lond.* **115**, 513–585 (1825).
- Carey, J. R., Liedo, P., Orozco, D. and Vaupel, J. W. Slowing of mortality rates at older ages in large medfly cohorts. *Science* **258**, 457–461 (1992).
- Ricklefs, R. E. Evolutionary theories of aging: Confirmation of a fundamental prediction, with implications for the genetic basis and evolution of life span. *Am. Nat.* **152**, 24–44 (1998).
- Vanfleteren, J. R., Vreese, A. D. and Braeckman, B. P. Two-parameter logistic and weibull equations provide better fits to survival data from isogenic populations *Caenorhabditis elegans* in axenic culture than does the Gompertz model. *J. Gerontol. Biol. Sci.* **53**, 393–403 (1998).
- Shoyama, T., Ozaki, T., Ishii, N., Yokota, S. and Suda, H. Basic principle of the lifespan in the nematode *C. elegans*. *Mech. Ageing Dev.* **128**, 529–537 (2007).
- Herndon, L. A., Schmeissner, P. J., Dudaronek, J. M., Brown, P. A., Listner, K. M., Sakano, Y., Paupard, M. C., Hall, D. H. and Drisco, M. Stochastic and genetic factors influence tissue-specific decline in ageing *C. elegans*. *Nature* **419**, 808–814 (2002).
- Estaquier, J. and Arnoult, D. CED-9 and EGL-1: A duo also regulating mitochondrial network morphology. *Mol. Cell* **21**, 730–732 (2006).
- Syntichaki, P., Troulinaki, K. and Tavernarakis, N. eIF4E function in somatic cells modulates ageing in *Caenorhabditis elegans*. *Nature* **445**, 922–926 (2007).
- Vaupel, J. W. and Yashin, A. I. Heterogeneity's ruses: Some surprising effects of selection on population dynamics. *Amer. Stat.* **39**, 176–185 (1895).
- Wu, D., Rea, S. L., Yashin, A. I. and Johnson, T. E. Visualizing hidden heterogeneity in isogenic populations of *C. elegans*. *Exp. Gerontol.* **41**, 261–270 (2006).
- Brenner, S. The genetics of *Caenorhabditis elegans*. *Genetics* **77**, 71–94 (1974).
- Gems, D. and Riddle, D. L. Genetic, behavioral and environmental determinants of male longevity in *Caenorhabditis elegans*. *Genetics* **154**, 1597–1610 (2000).
- Vaupel, J. W., Johnson, T. E. and Lithgow, G. J. Rates of mortality in populations of *Caenorhabditis elegans*. *Science* **266**, 826 (1994).
- Dillin, A., Hsu, A., Arantes-Oliveira, N., Lehrer-Graiwer, J., Hsin, H., Fraser, A. G., Kamath, R. S., Ahringer, J. and Kenyon, C. Rates of behavior and aging specified by mitochondrial function during development. *Science* **298**, 2398–2401 (2002).
- Hirabayashi, Y. and Inoue, T. Implications of hemopoietic progenitor cell kinetics and experimental leukemogenesis: Relevance to Gompertzean mortality as possible hematotoxicological endpoint. *Exp. Hemat.* **35**, 125–133 (2007).